FARADAY RESEARCH ARTICLE

# Optical Second-harmonic Generation Measurements of Molecular Adsorption and Orientation at the Liquid/Liquid Electrochenical Interface

**Roberta R. Naujok, Daniel A. Higgins, Dennis G. Hanken and Robert M. com***
*Department of Chemistry, University of Wisconsin-Madison, 1101 University ave., Madison, Wisconsin 53706, USA*

The surface-sensitive spectroscopic technique of optical second-harmonic generation (SHG) is applied to the *in situ* study of molecular adsorption at the interface between two immiscible electrolyte solutions (ITIES). The resonant SHG from molecules which exhibit a large non-linear optical response at a specific wavelength can be used to measure the relative surface coverage of surfactants at the ITIES as a function of the external electrochemical parameters. In addition, the polarization dependence of the resonant surface SHG can be used to estimate the average molecular orientation of adsorbates at the liquid/liquid electrochemical interface. As an example, the adsorption of the surfactant 4-(4'-dodecyloxyazobenzene)benzoic acid at the water/1,2-dichloroethane interface is characterized as a function of applied potential, surfactant concentration and aqueous pH with *in situ* resonant molecular SHG measurements. An analysis of the SHG data results in the determination of the local potential and surface pH experienced by the surfactant.

## 1. Introduction

The formation of adsorbed monolayers at liquid/liquid interfaces frequently plays a central role in many natural and synthetic chemical systems that are relevant in the fields of separation science, electrochemistry, environmental science and biology. To understand the function of these adsorbed monolayers completely, an intimate knowledge of the interface structure is required. For this reason, researchers from diverse scientific backgrounds have endeavoured to understand the adsorption, orientation, organization, transport and reactivity of both solvent and solute molecules at various liquid/liquid interfaces. One particular type of liquid/liquid interface which has been of interest since the turn of the century is the ITIES.[1] In the past 30 years, a great deal of information on the structure of the ITIES has been obtained from a combination of interfacial tension and electrochemical measurements.[2–8] However, to date there have been exceedingly few spectroscopic studies of molecular adsorption to the ITIES.[9–11] A major obstacle in the spectroscopic study of the liquid/liquid interface is the separation of the optical response of the interface from that of the adjacent bulk media.

Optical SHG is an inherently surface-selective and surface-sensitive process that overcomes this difficulty in signal separation.[12] The second-harmonic process converts two photons of frequency $\omega$ to one photon of frequency $2\omega$. In the electric dipole approximation, this process requires a non-centrosymmetric medium. For the case of an interface between two centrosymmetric media, such as the liquid/liquid interface, only the molecules which participate in the symmetry-breaking of the interface will contribute to the observed SHG. This symmetry requirement usually dictates that only the first few molecular monolayers at the interface are responsible for the entire surface second-harmonic response. It is this extreme surface selectivity that makes the SHG technique so useful for spectroscopic measurements at liquid/liquid interfaces, and has led to its application in many areas of surface science.[13–17]

At the ITIES, there are several possible molecular sources of surface SHG.[18] First, all of the solvent molecules and electrolyte ions at the interface will have a weak non-linear optical response. These 'non-resonant' contributions to the surface SHG are typically small, but can be observed; for example, Goh *et al.* have used non-resonant SHG to deduce the absolute orientation of water molecules at the air/water interface.[19] A second possible source of SHG from the liquid/liquid electrochemical interface is the symmetric-breaking induced by the interfacial electrostatic fields. This 'electric field-induced SHG' has been observed at semiconductor,[20,21] silica and metal[13] surfaces in contact with aqueous solutions, but has been observed to be weak at the ITIES.[22] A third, larger contribution to the SHG from liquid/liquid electrochemical interfaces can be obtained when the laser frequencies are tuned into resonance with an electronic transition of an adsorbed molecule. This large molecular surface second-harmonic response is sometimes referred to as 'resonant SHG',[23] and typically requires molecules which have been designed to provide a large non-linear optical response. This molecular response is described by the second-order molecular non-linear polarizability tensor, $\beta$, and can be calculated theoretically.[12,24–26] In addition, the polarization dependence of the resonant SHG response from a monolayer of adsorbed molecules will depend upon the average molecular orientation at the surface. We have recently published a series of resonant molecular SHG studies of surfactant adsorption, orientation and reaction at the liquid/liquid electrochemical interface.[9–11]

This article endeavours to provide an overview of the theory and methodology of surface SHG experiments for those scientists interested in applying this non-linear spectroscopic technique to liquid/liquid interfaces. The experimental details of the technique as well as the basic calculations required for an analysis of the surface second-harmonic response and a determination of the average molecular orientation at the interface are presented. As an example, the acid–base chemistry of carboxylic acid-terminated surfactants adsorbed to the water/1,2-dichloroethane (DCE) electrochemical interface is studied in detail with resonant molecular SHG measurements.

## 2. Experimental

A block diagram of the apparatus for the surface SHG experiment is shown in Fig. 1A. Since the surface SHG is

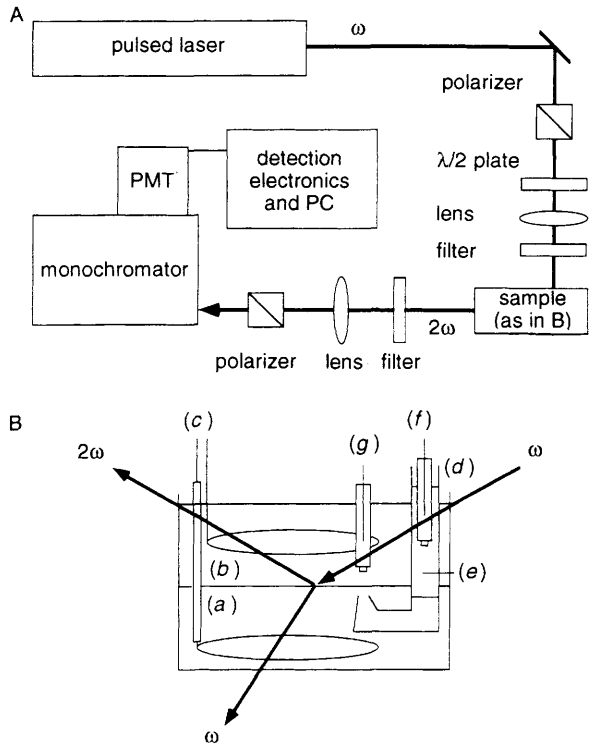


**Fig. 1** A, SHG experimental apparatus. B, Electrochemical cell used for interfacial tension and SHG measurements of the ITIES. The components of the cell are labelled as follows: (*a*) 1,2-dichloroethane (DCE) solution, (*b*) aqueous solution, (*c*) platinum counter-electrodes, (*d*) Luggin capillary for the organic phase reference electrode, (*e*) aqueous phase filling solution for the organic phase Luggin capillary, (*f*) and (*g*) Ag/AgCl reference electrodes. The fundamental beam is incident on the air/water interface at an angle of 60° which corresponds to an incident angle of 38° at the water/DCE interface.

proportional to the square of the incident light intensity, a high-power pulsed laser is typically employed as the light source. The most commonly used lasers are either ns or ps pulsed dye/Nd : YAG laser systems that can create tunable light from 550 to 850 nm. For example, the experiments described in this paper were performed with a dye laser that was pumped with a ns Nd : YAG laser (Quantel, Model NY-580) to provide light at 730 nm (10 Hz repetition rate, 10 ns pulse width, 5 mJ pulse energy).[27] The polarization of the incident fundamental light is controlled with a polarizer–half-wave plate combination prior to the sample. The incident polarization can be set to p-polarization (parallel to the plane of incidence and defined as 0°), s-polarization (polarized perpendicular to the plane of incidence and defined as 90°), or some intermediate polarization angle $\gamma$ ($0 < \gamma$/degree $< 90$). A coloured-glass cutoff filter is placed in the beam path immediately before the sample to remove any second-harmonic light generated by optics prior to the surface. The second-harmonic light generated in reflection at the ITIES is collected through a cutoff filter (to remove residual laser fundamental light), a collimating lens and a polarizer that is set to select either s-polarized or p-polarized SHG from the surface. The second-harmonic beam is then focused into a monochromator in order to eliminate any possible fluorescence from two-photon absorption. The second-harmonic light is subsequently detected with a photomultiplier and a boxcar averaging system, as described elsewhere.[27] Conversion efficiencies in these surface SHG experiments are normally very small (of the order of $10^{-12}$%) and the resultant SHG signal from the ITIES typically ranges from 0.2 to 80 counts $s^{-1}$, depending on the laser intensity, surface coverage and non-linear response of the adsorbed molecules.

A schematic diagram of the sample arrangement for the ITIES experiments is shown in Fig. 1B. The fundamental laser beam is incident on the air/water surface at an angle of 60° from the surface normal, corresponding to an angle of 38° at the water/DCE interface. The laser spot size on the ITIES is *ca.* 1 $mm^2$, corresponding to a power density of 40 MW $cm^{-2}$. The usable range of surface power densities in these SHG measurements is limited at the low end by the non-linear susceptibility of the adsorbates and at the high end by the damage threshold of the interface. A good method for selecting a safe power level while simultaneously verifying the non-linear nature of the optical response is to demonstrate that the observed SHG signal is proportional to the square of the incident laser intensity.

The two electrolyte solutions employed in formation of the ITIES were a 50 mmol $dm^{-3}$ NaCl aqueous solution made from Millipore-filtered water and a 1 mmol $dm^{-3}$ tetrabutylammonium tetraphenylborate (TBATPB) DCE solution made from SpectrAR grade (Mallinckrodt) 1,2-dichloroethane obtained from Baxter Scientific. All salts were obtained from Fluka Chemical Corp. (puriss grade) and were used as received. A four-electrode potentiostat was used to control the potential and to measure the current across the liquid/liquid interface.[9] Two platinum (DF Goldsmith) loops were used as the counter-electrodes in the aqueous and organic phases, and two Ag/AgCl/saturated NaCl electrodes were used as reference electrodes. The reference electrodes were placed in Luggin capillaries positioned near the ITIES to minimize IR drop problems. As in previous ITIES measurements,[28] the Luggin capillary in the organic phase was half-filled with DCE and then topped off with a 25 mmol $dm^{-3}$ tetrabutylammonium chloride (TBACl) aqueous solution in which the second Ag/AgCl electrode resided. The electrochemical system can be described as follows:

$$\text{Ag/AgCl}\|\text{25 mmol dm}^{-3}\text{ TBACl in H}_2\text{O}|\text{1 mmol dm}^{-3}$$
$$\text{TBATPB in DCE}\,*|*$$
$$\text{50 mmol dm}^{-3}\text{ NaCl in H}_2\text{O}\|\text{AgCl/Ag}$$

where the starred interface (*|*) is the liquid/liquid interface of interest. Following the convention of previous authors, the potential applied with the potentiostat to this electrochemical cell is denoted as $E_w - E_d$. Because the dipole layer at the water/DCE interface has been measured to be quite small (<5 mV),[29] $E_w - E_d$ is approximately equal to the Galvani potential difference between the two phases, $E_w - E_d \approx \Delta\phi_{wd} = \phi_w - \phi_d$.

The surfactant molecule 4-(4′-dodecyloxyazobenzene) benzoic acid (DBA) was synthesized in our laboratory,† and its structure and purity were verified by NMR and mass spectrometry. Prior to the SHG experiments, the two immiscible solutions were pre-equilibrated by mixing in a separatory funnel. The aqueous phase consisted of 25 $cm^3$ of a 50 mmol $dm^{-3}$ NaCl buffered aqueous solution and the organic phase was 25 $cm^3$ of a 1 mmol $dm^{-3}$ TBATPB, $Y$ ($Y$ = 0–50) μmol $dm^{-3}$ DBA–DCE solution. The pH of the buffered aqueous solutions varied from 5.0 to 9.8 and was adjusted with 10 mmol $dm^{-3}$ $Na_2HPO_4$ and either HCl or NaOH. UV–VIS experiments demonstrated that partitioning of the DBA as either the neutral or the anionic species into the aqueous phase was negligible (<0.5%). Once in place, the liquid/liquid sample was allowed to sit at open circuit for at least 1 h in order to permit the surfactant adsorbed at the ITIES to reach

† DBA was prepared using the Williamson ether synthesis with ethyl(4-hydroxy)azobenzene benzoate and iodododecane. The ethyl ester was cleaved by KOH in ethanol and acidified to produce the acid DBA. Further details will be presented in a future publication.

equilibrium. To complement the spectroscopic experiments, interfacial tension measurements were made by the Wilhelmy method with a NIMA Technologies electronic balance and a Teflon plate using a procedure described elsewhere.[9,30]

## 3. Molecular Non-linear Polarizability Calculations

The use of resonant SHG from surfactant molecules adsorbed to the ITIES requires selection of compounds with a sufficiently large non-linear optical response at a specific fundamental wavelength. As mentioned above, the sign and magnitude of this molecular SHG response are described by the second-order molecular non-linear polarizability tensor, $\boldsymbol{\beta}$. Using perturbation theory, the components of $\boldsymbol{\beta}$ can be expressed in terms of the molecular energies and wavefunctions:[24,26]

$$\begin{aligned}\beta_{ijk} + \beta_{ikj} = \frac{-e^3}{4h^2} \sum_{n,n'=g}^{N} & [(r^j_{gn'} r^i_{n'n} r^k_{ng} + r^k_{gn'} r^i_{n'n} r^j_{ng}) \\ & \times \{(\omega_{n'n} - 2\omega + i\Gamma_{n'n})^{-1}[(\omega_{ng} + i\Gamma_{ng})^{-1} \\ & - (\omega_{n'g} - \omega + i\Gamma_{n'g})^{-1}] \\ & \pm (\omega_{n'n} - 2\omega - i\Gamma_{n'n})^{-1}[(\omega_{ng} + \omega + i\Gamma_{ng})^{-1} \\ & - (\omega_{n'g} - \omega - i\Gamma_{n'g})^{-1}]\}] \\ & + \{(r^j_{gn'} r^k_{n'n} r^i_{ng} + r^k_{gn'} r^j_{n'n} r^i_{ng}) \\ & \times [(\omega_{n'g} - \omega + i\Gamma_{n'g})^{-1}(\omega_{ng} - 2\omega + i\Gamma_{ng})^{-1} \\ & \pm (\omega_{n'g} - \omega - i\Gamma_{n'g})^{-1}(\omega_{ng} - 2\omega - i\Gamma_{ng})^{-1}]\} \\ & + \{(r^i_{gn'} r^j_{n'n} r^k_{ng} + r^i_{gn'} r^k_{n'n} r^j_{ng}) \\ & \times [(\omega_{ng} + \omega - i\Gamma_{ng})^{-1}(\omega_{n'g} + 2\omega - i\Gamma_{n'g})^{-1} \\ & \pm (\omega_{ng} + \omega + i\Gamma_{ng})^{-1}(\omega_{n'g} + 2\omega + i\Gamma_{n'g})^{-1}]\} \quad (1)\end{aligned}$$

where $\beta_{ijk}$ is the tensor element referenced to the molecular coordinate axes $i, j$ and $k$; the sum to $N$ is the double summation over all states $n$ and $n'$; $\omega$ is the incident laser frequency; $\omega_{ng}$ is the frequency difference between excited state $n$ and the ground state g; $\Gamma_{ng}$ is the decay time (approximately the dephasing time) from excited state $n$ to the ground state; and $\boldsymbol{r}_{ng}$ is the transition dipole matrix element between states $n$ and g. Excited-state lifetimes ($\Gamma_{nn}$) and population feeding terms have been neglected in this equation. Where the notation '$\pm$' occurs in the equation, the '+' signs are used to obtain the in-phase (real) components of $\boldsymbol{\beta}$ and the '−' signs are used to obtain the 90° out-of-phase (imaginary) components.

The complexities involved in calculating $\boldsymbol{\beta}$ from eqn. (1) are obvious. Fortunately, the salient features of the molecular second-harmonic response can be obtained from a simple two-level model where one considers only a ground and a single optically accessible excited state (Fig. 2). The elements of the non-linear polarizability tensor are then given by eqn. (2):[31]

$$\beta_{ijk} = \frac{-e^3}{2h^2}\left[\frac{\Delta r^i_n r^j_{ng} r^k_{ng}}{\omega^2_{ng} - \omega^2} + r^i_{ng}(r^j_{ng}\Delta r^k_n + \Delta r^j_n r^k_{ng}) \times \frac{\omega^2_{ng} + 2\omega^2}{(\omega^2_{ng} - 4\omega^2)(\omega^2_{ng} - \omega^2)}\right] \quad (2)$$

where $\Delta \boldsymbol{r}_n$ is the difference in the permanent dipole moment between excited state $n$ and the ground state, g. Note the following characteristics of the second-harmonic response from this two-level system:

(i) $\boldsymbol{\beta}$ has resonances at two wavelengths: once when the laser frequency $\omega$ is equal to $\omega_{ng}$, and a second time when the laser frequency is equal to $\omega_{ng}/2$ (see Fig. 2). This second condition corresponds to the second-harmonic wavelength being in resonance with an optical transition in the molecule, and is particularly useful since the SHG enhancement can be obtained at a wavelength where there is virtually no absorption of the incident laser power. SHG measurements which solely utilize resonances at twice the laser frequency avoid the problems of photobleaching, burning and fluorescence. An additional advantage of such measurements is that molecules with resonances in the near-UV can be monitored with the use of readily available visible dye lasers.

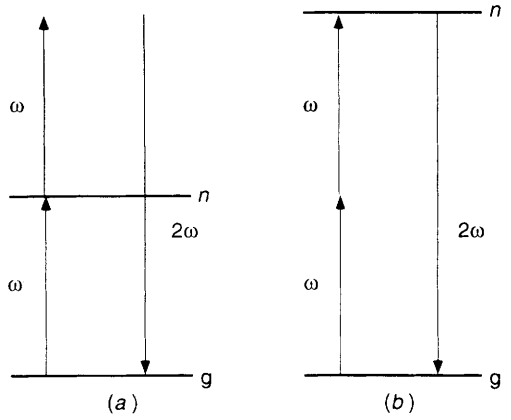


**Fig. 2** Two-state model for resonant molecular SHG. State g is the ground state for the SHG-active molecule and state $n$ is a single optically accessible excited state. Case (*a*) is where a molecular resonance occurs at the fundamental wavelength ($\omega = \omega_{ng}$), and case (*b*) is where a molecular resonance occurs at the second-harmonic wavelength ($2\omega = \omega_{ng}$). Case (*b*) is the preferred situation for surface SHG measurements since it avoids problems with photobleaching or saturation from the high powered fundamental probe beam.

(ii) The elements of $\boldsymbol{\beta}$ in eqn. (2) are proportional to the elements of the change in the permanent dipole moment of the molecule from the ground to excited state, $\Delta \boldsymbol{r}_n$. Therefore, molecules with strong charge-transfer transitions are typically employed as SHG-active compounds.[32–34] These molecules usually contain an extended $\pi$-electronic structure with an electron-donating group at one end of the molecule (*e.g.* OH, $NH_2$) and an electron-accepting group at the other end (*e.g.* $NO_2$, carboxylic acid).

(iii) $\boldsymbol{\beta}$ is a tensor formed by the direct product of the vectors $\boldsymbol{r}_{ng}$ and $\Delta \boldsymbol{r}_n$. Thus, any component of $\boldsymbol{\beta}$ that involves the axis perpendicular to the plane defined by $\boldsymbol{r}_{ng}$ and $\Delta \boldsymbol{r}_n$ will be zero. If $\boldsymbol{r}_{ng}$ and $\Delta \boldsymbol{r}_n$ are collinear, then only one tensor element, defined as $\beta_{zzz}$, will be non-zero. Most of the previous studies that determined an average molecular orientation from SHG measurements assumed that the non-linear response of the adsorbed molecules could be described by a single dominant molecular non-linear polarizability tensor element.[23,35] This assumption has been relaxed in a series of recent papers.[9,10,26,36–38]

The simple two-state model provides a clear description of the non-linear polarizability for small molecules in spectral regions near a single electronic resonance. However, for larger dye molecules with many low-energy electronic transitions, and even for smaller molecules very close to resonance, the two-state model breaks down and a more complete calculation utilizing eqn. (1) is required. In these more complicated systems, the calculation can be simplified for most aromatic molecules by assuming that only the $\pi$-electronic structure contributes to the molecular non-linear polarizability in the UV–VIS spectroscopic region. For these molecules, a $\pi$-electron calculation such as the method of Pople–Pariser–Parr (PPP), can be used to obtain the ground- and excited-state energies and wavefunctions for the molecule.[39,40] The elements of $\boldsymbol{\beta}$ can then be calculated from eqn. (1).[26] These non-linear polarizability calculations have been

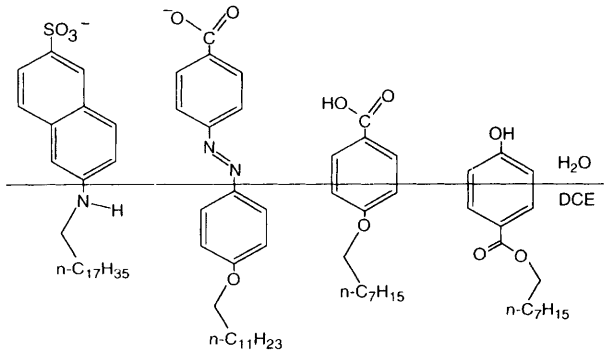


**Fig. 3** Various SHG-active surfactants employed in the ITIES experiments: ONS, 2-(*n*-octadecylamino)naphthalene-6-sulfonate; DBA, 4-(4'-dodecyloxyazobenzene)-benzoic acid; OBA, 4-octyloxybenzoic acid and OHB, *n*-octyl-4-hydroxybenzoate. The fundamental wavelength for resonant molecular SHG studies is listed for each molecule.

used by other authors in the examination of non-linear active materials;[25,41–43] for our purposes the calculations allow us to select and design appropriate SHG probe molecules for the ITIES experiments. Some of the SHG-active surfactant molecules that we have employed at the ITIES are displayed in Fig. 3 along with their resonant fundamental wavelengths.

Two examples of SHG-active surfactant molecules that are adsorbed to the ITIES are the electronically similar 4-octyloxybenzoic acid (OBA) and *n*-octyl-4-hydroxybenzoate (OHB) (see Fig. 3).[10] The results of a non-linear polarizability calculation for OBA and OHB are plotted in Fig. 4, and

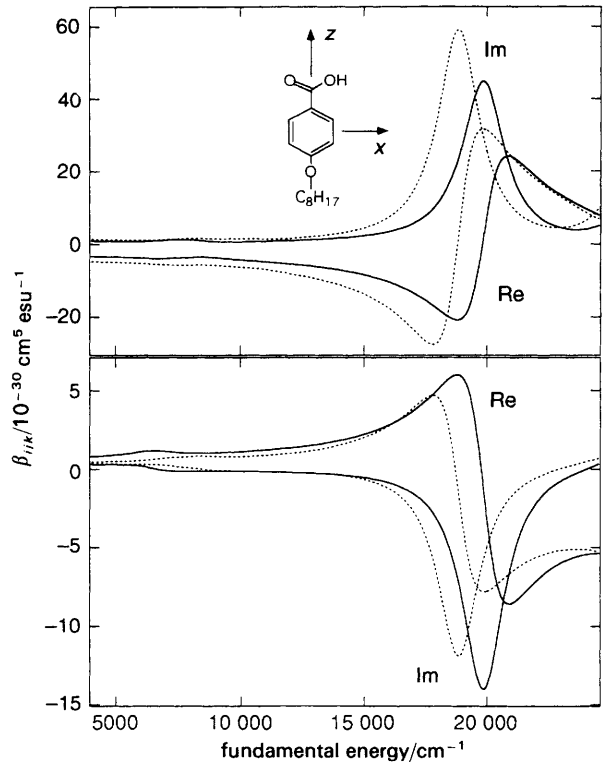


**Fig. 4** Semi-empirical $\pi$-electron molecular non-linear polarizability calculations for the SHG-active surfactant molecules OBA and OHB. The tensor elements $\beta_{zzz}$ and $\beta_{zxx}$ were found to be the dominant elements where $z$ and $x$ are defined with respect to the molecular symmetry axis as depicted for OBA in the figure. Both the real (Re) and imaginary (Im) components are shown for $\beta_{zzz}$ (top) and $\beta_{zxx}$ (bottom) for OBA (——) and OHB (– – –).

show that these two molecules have large non-linear polarizabilities at a fundamental wavelength of *ca.* 532 nm. In these molecules, both $\beta_{zzz}$ and $\beta_{zxx}$ are active when on resonance. Owing to the approximate nature of the semi-empirical calculations, these results are not used to quantify the relative magnitudes of the two tensor elements. They do, however, provide an excellent tool for selecting molecules on the basis of the overall magnitude of $\beta$ and determining the major non-zero molecular non-linear polarizability tensor elements.

## 4. Surface SHG Polarization Analysis and Molecular Orientation Measurements

While the previous section details the criteria for a large non-linear response from a single molecule, the SHG from a liquid/liquid surface is composed of the contributions from many molecules in various orientations and environments. This composite-surface response is described by the surface non-linear susceptibility tensor, $\chi^{(2)}$. A measure of the number of molecules at the surface can be obtained from the overall magnitude of $\chi^{(2)}$ and is discussed further in Section 5. Molecular orientation information can also be extracted from $\chi^{(2)}$ through an analysis of the polarization dependence of the surface SHG.[14,15,37,44,45] This information is obtained by relating the various elements of the surface non-linear susceptibility tensor $\chi^{(2)}_{IJK}$ (hereafter denoted $\chi_{IJK}$, where $I$, $J$ and $K$ refer to the cartesian axes defined relative to the surface) to averages of the elements of the individual molecular non-linear polarizability tensor $\beta_{ijk}$ (where $i$, $j$ and $k$ refer to axes defined relative to the molecular symmetry axis). In the first part of this section we describe how to obtain the elements $\chi_{IJK}$ from the polarization dependence of the surface SHG signal, and then in the second part we show how to use the relations between $\chi_{IJK}$ and $\beta_{ijk}$ to obtain an average orientation angle for the adsorbed molecules.

### 4.1 Elements of $\chi^{(2)}$

When adsorbed to a surface, a monolayer of SHG-active molecules collectively responds to an incident laser light field at frequency $\omega$ to create an induced non-linear polarization at frequency $2\omega$. This non-linear polarization in turn leads to the coherent generation of light at the second-harmonic wavelength. The intensity of SHG from the interface, $I(2\omega)$, is related to $\chi^{(2)}$ by eqn. (3):[15,46]

$$I(2\omega) = \frac{32\pi^3\omega^2 \sec^2\theta_{2\omega}}{c^3} |\boldsymbol{e}(2\omega)\cdot\boldsymbol{\chi}^{(2)}:\boldsymbol{e}(\omega)\boldsymbol{e}(\omega)|^2 I(\omega)^2 \quad (3)$$

where $I(\omega)$ is the intensity of the incident laser light, $\theta_{2\omega}$ is the angle from the surface normal at which the SHG signal occurs, the vectors $\boldsymbol{e}(\omega)$ and $\boldsymbol{e}(2\omega)$ describe the polarization state and Fresnel factors for the fundamental and second-harmonic light fields at the surface, and all other symbols have their usual meaning.

The components of $\boldsymbol{e}(\omega)$ and $\boldsymbol{e}(2\omega)$ depend upon the exact experimental geometry employed in the surface SHG experiments. The components of $\boldsymbol{e}(\omega)$ and $\boldsymbol{e}(2\omega)$ for the ITIES experiments presented in this paper are given by:[37]

$$\begin{aligned}
e_x(\omega) &= t_1^{\parallel}(\omega)[1 - r_2^{\parallel}(\omega)]\cos\theta_\omega \\
e_y(\omega) &= t_1^{\perp}(\omega)[1 + r_2^{\perp}(\omega)] \\
e_z(\omega) &= t_1^{\parallel}(\omega)[1 + r_2^{\parallel}(\omega)]\sin\theta_\omega \\
e_x(2\omega) &= -t_1^{\parallel}(2\omega)t_2^{\parallel}(2\omega)\cos\theta_{2\omega} \\
e_y(2\omega) &= t_1^{\perp}(2\omega)t_2^{\perp}(2\omega) \\
e_z(2\omega) &= t_1^{\parallel}(2\omega)t_2^{\parallel}(2\omega)\sin\theta_{2\omega}
\end{aligned} \quad (4)$$

In eqn. (4), $\theta_\omega$ is the angle of incidence for the fundamental laser light at the water/DCE interface (38°), $t_1^{\parallel}$ and $t_1^{\perp}$ are the Fresnel transmission coefficients through the first (air/water) interface for p- and s-polarized light, respectively, and $r_2^{\parallel}$ and $r_2^{\perp}$ are the Fresnel reflection coefficients for the second (water/DCE) interface. These equations were derived following the method of Mizrahi and Sipe.[46] The Fresnel coefficients are usually calculated from the tabulated optical constants for the bulk media, assuming that any correction due to the presence of the adsorbed monolayer can be neglected. Explicit equations for $e(\omega)$ and $e(2\omega)$ that apply to different experimental geometries can be found in other papers.[15,46]

If the SHG from the adsorbed monolayer is invariant during rotation of the sample about the surface normal (defined as the $Z$ axis), then the molecules within the laser spot are randomly oriented in the azimuthal direction and $\chi^{(2)}$ has only three unique non-zero elements: $\chi_{XXZ}$, $\chi_{ZXX}$ and $\chi_{ZZZ}$.[12] The intensity of the s- and p-polarized SHG signal [$I_s(2\omega)$ and $I_p(2\omega)$, respectively] can then directly related to these elements:

$$I_s(2\omega) \propto |a_1\chi_{XXZ} \sin 2\gamma|^2 I(\omega)^2 \quad (5)$$

$$I_p(2\omega) \propto |(a_2\chi_{XXZ} + a_3\chi_{ZXX} + a_4\chi_{ZZZ})\cos^2\gamma + a_5\chi_{ZXX}\sin^2\gamma|^2 I(\omega)^2 \quad (6)$$

where $\gamma$ is the polarization angle of the incident light ($\gamma = 0°$ for p-polarized light and 90° for s-polarized light) and the $a_i$ terms describe the electric fields in the monolayer. The $a_i$ terms for the water/DCE ITIES system presented in this paper are given by:

$$\begin{aligned} a_1 &= e_y(\omega)e_z(2\omega)[\varepsilon_w(\omega)/\varepsilon'(\omega)] \\ a_2 &= 2e_x(\omega)e_z(\omega)e_x(2\omega)[\varepsilon_w(\omega)/\varepsilon'(\omega)] \\ a_3 &= |e_x(\omega)|^2 e_z(2\omega)[\varepsilon_d(2\omega)/\varepsilon'(2\omega)] \\ a_4 &= |e_z(\omega)|^2 e_z(2\omega)[\{\varepsilon_w(\omega)^2\varepsilon_d(2\omega)\}/\{\varepsilon'(\omega)^2\varepsilon'(2\omega)\}] \\ a_5 &= |e_y(\omega)|^2 e_z(2\omega)[\varepsilon_d(2\omega)/\varepsilon'(2\omega)] \end{aligned} \quad (7)$$

where the relative permittivities for water and DCE at the fundamental and second-harmonic frequencies are taken from the tabulated values:[47]† $\varepsilon_w(\omega) = 1.77$, $\varepsilon_w(2\omega) = 1.85$, $\varepsilon_d(\omega) = 2.04$ and $\varepsilon_d(2\omega) = 2.13$. The relative permittivities of the monolayer at the fundamental and the second-harmonic wavelengths, $\varepsilon'(\omega)$ and $\varepsilon'(2\omega)$, can be estimated from bulk values, determined directly by ellipsometry, or approximated by assuming a monolayer thickness and using a Kramers–Kronig analysis of the optical absorption spectrum.[26,36] Guyot-Sionnest *et al.* have stressed the need for an independent measurement of $\varepsilon'(\omega)$ and $\varepsilon'(2\omega)$ in order to obtain a true molecular orientation measurement.[48]

As an example of the polarization dependence of the surface SHG signal, the experimentally determined values for $I_p(2\omega)$ and $I_s(2\omega)$ for a monolayer of the surfactant DBA adsorbed to the water/DCE ITIES are plotted in Fig. 5 as a function of $\gamma$. Virtually no SHG was observed from the interface in the absence of DBA. From these data, the relative magnitudes of the various $\chi^{(2)}$ elements for the monolayer can be obtained *via* eqn. (5) and (6). The solid lines are the best fits to the data, and correspond to a ratio of magnitudes of the three tensor elements $\chi_{ZZZ}$, $\chi_{XXZ}$ and $\chi_{ZXX}$ of 6.80 : 1.03 : 1.00. From this ratio an average molecular orientation can be obtained *via* the procedure outlined below.

† The relative permittivity for DCE at the second-harmonic wavelength was calculated by increasing the tabulated $\varepsilon_d(\omega)$ by the same percentage as the change in the relative permittivity of water.

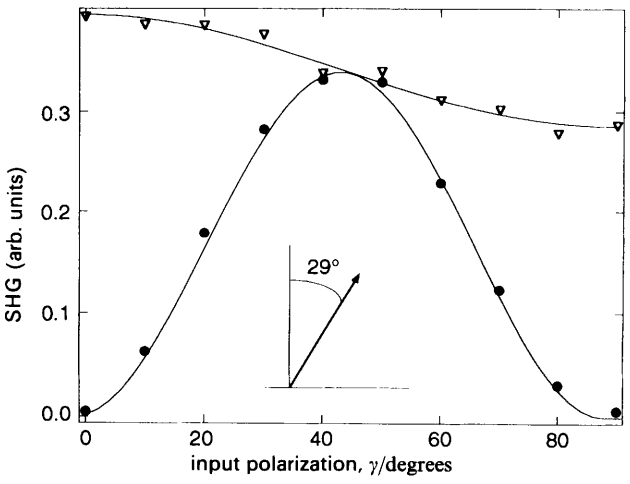


**Fig. 5** Polarization dependence of the resonant molecular SHG response from an adsorbed DBA monolayer at the water/DCE electrochemical interface. The $pH_w$ of the aqueous phase is 8.0, the DBA concentration in the DCE is 20 μmol $dm^{-3}$ and the potential is at open circuit. The p-polarized (●) and s-polarized (▽) SHG from the monolayer are plotted as a function of input polarization, where 0° corresponds to p-polarized and 90° to s-polarized fundamental light. The solid lines are the theoretical fits used to determine values for the surface non-linear susceptibility tensor elements $\chi_{ZXX}$, $\chi_{XXZ}$ and $\chi_{ZZZ}$.

### 4.2 Molecular Orientation Calculation

Once the elements of $\chi^{(2)}$ have been determined, they can be related to the elements of the molecular non-linear polarizability tensor ($\beta_{ijk}$) by the molecular orientation distribution function. This mathematical relationship can be described as the average of the product of three direction cosines, $R_{Xx}$, between the laboratory and molecular coordinate systems:[49]

$$\begin{aligned} \chi_{IJK} &= N_s \sum \langle R_{Ii}R_{Jj}R_{Kk}\rangle\beta_{ijk} \\ &= N_s \sum \langle F_{IJKijk}(\xi, \theta, \alpha)\rangle\beta_{ijk} \end{aligned} \quad (8)$$

where $N_s$ is the surface concentration of adsorbed molecules. The product of the direction cosines in eqn. (8) can be expressed as the molecular orientation distribution function, $F_{IJKijk}(\xi, \theta, \alpha)$, where the molecular angles $\xi$, $\theta$ and $\alpha$ are defined as in Fig. 6. As mentioned above, we will only consider cases in which the SHG from the surface does not depend upon the azimuthal angle $\xi$, which implies that the molecules are oriented randomly about the surface normal and that $F_{IJKijk}$ can be integrated over all $\xi$. Further simplification of $F_{IJKijk}$ depends upon which tensor elements dominate the molecular non-linear polarizability tensor. As shown

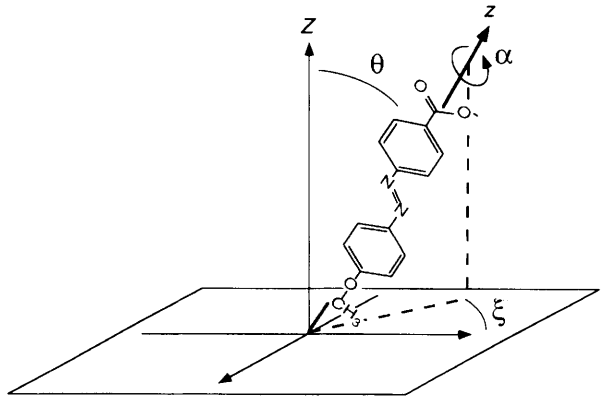


**Fig. 6** Definition of the angles $\alpha$, $\xi$ and $\theta$ employed in the molecular orientation calculation. The surface normal is defined as the $Z$-axis.

in section 3, the relative magnitudes of the various $\beta_{ijk}$ elements depend upon the structure of the molecule and can be identified with the semi-empirical non-linear polarizability calculations. The orientation analysis methodology for a variety of different combinations of contributing $\boldsymbol{\beta}$ elements is documented elsewhere.[37]

As an example, the surfactant molecules OBA and OHB possess only two significant $\boldsymbol{\beta}$ elements, $\beta_{zzz}$ and $\beta_{zxx}$ (see Fig 4), all other tensor elements being at least an order of magnitude less. In this case, the sum in eqn. (8) is reduced to two terms, and the relative magnitudes of $\beta_{zzz}$ and $\beta_{zxx}$ can be obtained from the experimentally determined values of the surface non-linear susceptibility tensor elements by eqn. (9):

$$\frac{\beta_{zxx}}{\beta_{zzz}} = 2\,\frac{\chi_{zxx} - \chi_{xxz}}{\chi_{zzz} + 2\chi_{xxz}} \tag{9}$$

Relative values of the $\chi^{(2)}$ elements for OBA were found to be $\chi_{zzz} : \chi_{zxx} : \chi_{xxz} = 4.79 : 1.34 : 1.00$, and for OHB were found to be $\chi_{zzz} : \chi_{zxx} : \chi_{xxz} = 3.13 : 1.26 : 1.00$. These both correspond to $\beta_{zxx}/\beta_{zzz}$ ratios of *ca.* 0.10.[10]

In addition to the $\beta_{zxx}/\beta_{zzz}$ ratio, an orientation parameter, $D$, that is related to the elements of $\chi^{(2)}$ can be derived from eqn. (8):

$$D = \frac{\langle\cos^3\theta\rangle}{\langle\cos\theta\rangle} = \frac{\chi_{zzz} - \chi_{zxx} + \chi_{xxz}}{\chi_{zzz} + 3\chi_{xxz} - \chi_{zxx}} \tag{10}$$

The derivation of this orientation parameter assumes a random distribution in $\alpha$ for the molecules adsorbed to the water/DCE interface, and contributions from the $\beta_{zxx}$ and $\beta_{zzz}$ tensor elements only. From the $\chi^{(2)}$ element ratios for OBA and OHB, the orientation parameter $D$ was calculated to be 0.69 and 0.59, respectively. Assuming that the distribution in $\theta$ is narrow enough so that $\langle\cos^3\theta\rangle \approx \cos^3\langle\theta\rangle$ and $\langle\cos\theta\rangle \approx \cos\langle\theta\rangle$, these results correspond to orientation angles $\langle\theta\rangle$ of 34° and 40° for OBA and OHB, respectively.[10] This assumption of a very narrow distribution in $\theta$ is somewhat unrealistic, and an alternative interpretation of the orientation parameter in terms of a Gaussian distribution of orientation angles $\theta$ has been suggested.[26]

A second example of an orientation measurement is the case of the azobenzene surfactant DBA adsorbed to the water/DCE interface. Using the $\chi^{(2)}$ element ratios for DBA listed above in eqn. (9) results in a $\beta_{zxx}/\beta_{zzz}$ ratio for DBA of 0.008. Since this ratio is so small, it is reasonable to disregard the second tensor element $\beta_{zxx}$, and analyse the DBA data using only a single tensor element, $\beta_{zzz}$. As eqn. (9) suggests, when $\beta_{zzz}$ is the only non-zero tensor element, then $\chi_{zxx} = \chi_{xxz}$, and the molecular orientation distribution function as described by eqn. (8) reduces to:

$$\chi_{zxx} = \chi_{xxz} = \tfrac{1}{2}N_s\langle\cos\theta\sin^2\theta\rangle\beta_{zzz} \tag{11}$$

$$\chi_{zzz} = N_s\langle\cos^3\theta\rangle\beta_{zzz} \tag{12}$$

In the case of a single dominant $\beta_{zzz}$, the relationship between $D$ and the $\chi^{(2)}$ elements [eqn. (10)] reduces to the following simpler form:

$$D = \frac{\langle\cos^3\theta\rangle}{\langle\cos\theta\rangle} = \frac{\chi_{zzz}}{\chi_{zzz} + 2\chi_{xxz}} \tag{13}$$

The values of the $\chi^{(2)}$ element ratios for DBA at the water/DCE interface result in an orientation parameter, $D$, of 0.77. This corresponds to an average angle of 29° from the surface normal (assuming a narrow distribution in the angle $\theta$). The expression for $D$ in eqn. (13) does not depend upon a random orientation in the molecular angle $\alpha$.[35] In addition, when $\beta_{zzz}$ is the only contributing tensor element, only one of the monolayer relative permittivities, $\varepsilon'(\omega)$ or $\varepsilon'(2\omega)$, need be known. Since $\chi_{zxx} = \chi_{xxz}$, it is possible to calculate a value for the second relative permittivity from the experimental data. This methodology for incorporation of the monolayer relative permittivities into the orientation calculation has been discussed in detail by Zhang *et al.*[44]

## 5. Surface Coverage Measurements

While the relative magnitudes of the elements of the surface susceptibility tensor $\chi^{(2)}$ depend upon the average molecular orientation at the interface, all of the $\chi^{(2)}$ elements are proportional to the surface concentration of SHG-active molecules, $N_s$ [see eqn. (8)]. Since the SHG from the interface is proportional to $|\chi^{(2)}|^2$ [see eqn. (3)], this implies that if there is no change in the average molecular orientation (*i.e.* no change in the polarization dependence of the SHG), the SHG from the interface will vary as the square of the surface concentration. Thus, relative changes in the surface coverage of a chromophore at the interface can be extracted from changes in the square root of the surface second-harmonic response. This relationship has been used previously to monitor surface coverage at a variety of interfaces,[13] including the ITIES.[9] Other methods such as surface tension and differential capacitance measurements can also be used to determine the surface coverage of adsorbates at the ITIES, but these techniques do not possess any molecular specificity. In contrast, the SHG technique can be used to measure the surface coverage of an SHG-active surfactant coadsorbed at the ITIES with other compounds as long as the surface SHG at a given wavelength is in resonance with only one particular molecule.

SHG measurements at the ITIES can be used to monitor changes in the surface coverage of a compound as a function of bulk concentration, pH of the aqueous phase, and the potential across the interface. For example, changes in the relative surface coverage with applied potential for the anionic surfactant ONS (see Fig. 3) at the water/DCE ITIES have been obtained from the potential dependence of the resonant SHG from the surface and are plotted in Fig. 7.[9] In this analysis, we have assumed that the highest SHG levels correspond to an adsorbed monolayer with the maximum ONS surface coverage $N_s^\circ$, and have defined the relative surface coverage as $\theta = N_s/N_s^\circ$. The polarization dependence of the surface SHG signal did not vary as a function of

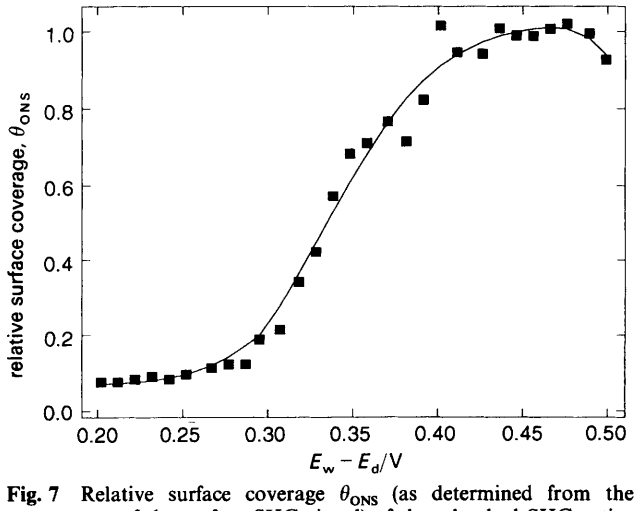


**Fig. 7** Relative surface coverage $\theta_{ONS}$ (as determined from the square root of the surface SHG signal) of the adsorbed SHG-active surfactant molecule ONS at the water/DCE ITIES as a function of the applied potential, $E_w - E_d$. The aqueous phase contained 20 μmol $dm^{-3}$ ONS, 50 mmol KCl $dm^{-3}$ and 25 mmol $dm^{-3}$ $Na_2HPO_4$ (pH 9) and the DCE contained 1 mmol $dm^{-3}$ TBATPB. Reprinted with permission from ref. 9.

applied potential. At potentials negative of the potential of zero charge (denoted as the pzc and equal to 0.25 V for this interface), there was no adsorption of the anion to the interface and therefore no SHG. At potentials positive of the pzc, ONS adsorption increased owing to the negative charge on the DCE side of the interface, and the surface SHG increased. Thermodynamic variables such as the free energy of adsorption of ONS to the interface were extracted from the shape of the adsorption curve.[9]

## 6. DBA Adsorption at the ITIES

As a final example of the study of adsorption at the liquid/liquid electrochemical interface with resonant molecular SHG, the changes in the relative surface coverage of the surfactant DBA at the water/DCE ITIES are examined as a function of concentration, pH and potential. Since DBA (Fig. 3) is a weak acid, it can exist at the liquid/liquid interface either as the neutral species or as the anion. As there is little difference in the UV–VIS absorption spectrum of the two, the resonant molecular SHG at 365 nm will detect either species. At an aqueous pH (denoted at $pH_w$) of 5.0, no change is observed in the surface tension of the water/DCE ITIES when 20 μmol $dm^{-3}$ of DBA is added to the DCE. However, at a $pH_w$ of 8.0, the surface tension drops by *ca.* 4 dyn $cm^{-1}$. From this drop, the adsorption of DBA to the interface with a surface coverage of *ca.* $10^{14}$ molecule $cm^{-2}$ can be estimated from the Gibbs equation.[9,50,51]

This $pH_w$ dependent adsorption of DBA to the water/DCE interface is verified with the resonant molecular SHG experiments. At a $pH_w \leqslant 5$, the surface SHG from the water/DCE ITIES for a 20 μmol $dm^{-3}$ DBA dichloroethane solution was negligible. As $pH_w$ was increased, the SHG signal from the interface rose to a maximum value at $pH_w \geqslant 9.5$. The polarization dependence of the surface SHG did not change with $pH_w$, indicating that no changes in average molecular orientation were observed. If the maximum surface SHG observed at the higher $pH_w$ values corresponds to the maximum surface coverage $N_s^\circ$, then a relative surface coverage $\theta = N_s/N_s^\circ$ can be obtained from the square root of the SHG signal at lower $pH_w$. A plot of $\theta$ as a function of $pH_w$ determined from the surface SHG signal at open circuit is shown in Fig. 8. The relative surface coverage reaches a value of one half at a $pH_w$ of 7.6, and the functional form of the $pH_w$ dependence suggests that at this concentration (20 μmol $dm^{-3}$ in DCE), the surface SHG signal is due to the presence of the deprotonated DBA anion at the interface with a $pK_a'$ of 7.6. However, this apparent $pK_a$ was found to vary as a function of the DBA concentration in the DCE phase.

In a second set of measurements, the surface SHG signal from the water/DCE ITIES at open circuit was obtained as a function of DBA concentration in the DCE phase (denoted as $[DBA]_d$) at a fixed $pH_w$ of 8.0. The relative surface coverage, $\theta$, as determined from the resonant molecular SHG measurements is plotted *vs.* $[DBA]_d$ in Fig. 9, and the form of the concentration dependence of $\theta$ is that of a Langmuir isotherm with an apparent adsorption coefficient, $K_{ads}'$, of $1.25 \times 10^5$ $dm^3$ $mol^{-1}$ at pH 8.0. Note that this apparent adsorption coefficient varied as a function of $pH_w$, in a manner similar to the apparent $pK_a$ values.

A model of the coupled surface and solution equilibria that describes the observed dependence of $\theta$ on $pH_w$ and $[DBA]_d$ is shown in Fig. 10. The neutral surfactant weak acid DBA is dissolved in the organic phase (DCE), and a certain amount is adsorbed to the liquid/liquid interface with a Langmuir adsorption coefficient, $K_{ads}$. The magnitude of $K_{ads}$ is already known to be small given the lack of SHG at low $pH_w$. The adsorbed surfactant will be deprotonated as a function of the surface pH (defined as $pH_s$) with a dissociation constant, $K_a$. In this model, the DBA anion does not exist to any appreciable extent in either the aqueous or the organic phases, but only at the surface ($A_s^-$). The presence of both forms of DBA (HA and $A^-$) in the aqueous phase was found to be less than 2% at the highest $pH_w$s; at the $pH_w$ values utilized for most of these experiments it was below the detection limits with UV–VIS absorption measurements, and estimated to be less than 0.5%. In addition, the presence of $A^-$ in the dichloroethane is likely to be small for a variety of reasons. Dissociation constants of weak acids in dichloroethane are known to be extremely small,[52] thus the amount of $A^-$ generated by

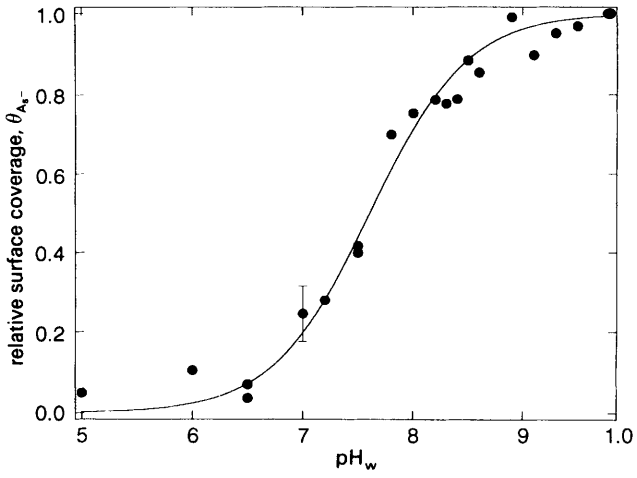


**Fig. 8** Relative surface coverage $\theta_{A_s^-}$ (as determined from the square root of the surface SHG signal) of the adsorbed SHG-active DBA anion at the water/DCE ITIES as a function of aqueous $pH_w$. The aqueous phase contained 50 mmol $dm^{-3}$ NaCl and 10 mmol $dm^{-3}$ $Na_2HPO_4$–HCl, and the DCE contained 20 μmol $dm^{-3}$ DBA and 1 mmol $dm^{-3}$ TBATPB. All measurements were made at open circuit. At a $pH_w \leqslant 6.5$, no adsorption of DBA is observed. As $pH_w$ is increased, the DBA surface coverage increases to a full monolayer ($\theta_{A_s^-} = 1$) with an effective $pK_a' = -\log(K_a K_{ads}[DBA]_d) = 7.6$. This effective $pK_a$ changed with the DBA concentration in the DCE. The solid line is a theoretical fit to eqn. (14), with $K_a K_{ads} = 1.25 \times 10^{-3}$.

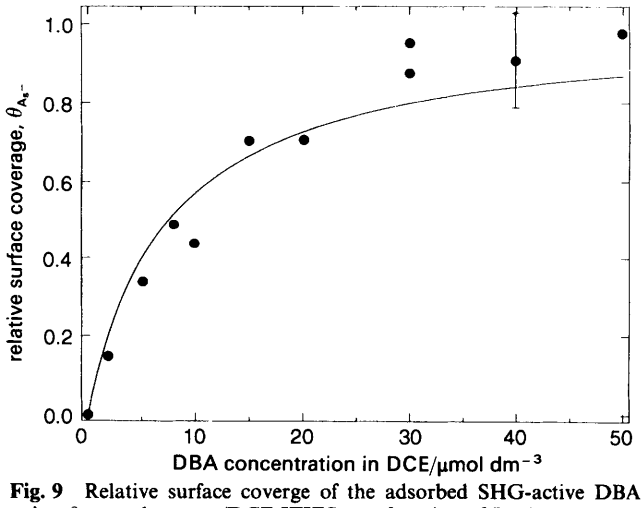


**Fig. 9** Relative surface coverge of the adsorbed SHG-active DBA anion $\theta_{A_s^-}$ at the water/DCE ITIES as a function of DBA concentration in the DCE. The aqueous phase contained 50 mmol $dm^{-3}$ NaCl, adjusted to a $pH_w$ of 8.0, and the DCE contained 1 mmol $dm^{-3}$ TBATPB and $Y$ ($Y$ = 0–50) μmol $dm^{-3}$ DBA. All measurements were made at open circuit. The solid line is a theoretical fit to eqn. (14) with a $K_a K_{ads} = 1.25 \times 10^{-3}$, and results in an apparent Langmuir adsorption coefficient $K_{ads}' = K_a K_{ads}/[H^+] = 1.25 \times 10^5$ $dm^3$ $mol^{-1}$. This apparent $K_{ads}'$ varied with $pH_w$.

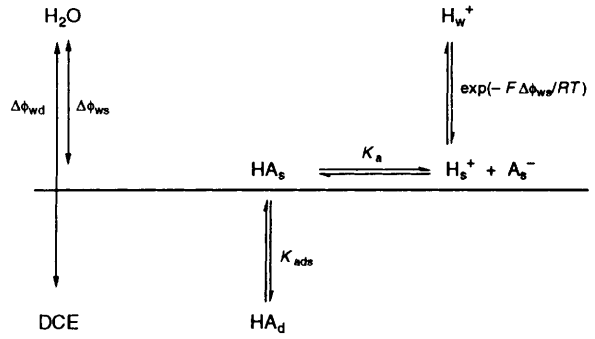


**Fig. 10** Equilibrium model of the DBA adsorption to the water/DCE ITIES. Neutral DBA molecules (HA) are present in the DCE and can adsorb weakly to the liquid/liquid interface. At the surface, the DBA can be deprotonated at sufficiently high interfacial pH (defined as $pH_s$) to form the anion, $A_s^-$. The interfacial $pH_s$ is controlled by the aqueous pH (defined as $pH_w$) and the potential drop $\Delta\phi_{ws}$ from the aqueous phase to the interface. This potential difference is some fraction of the total potential drop across the interface, $\Delta\phi_{wd}$. Note that the DBA anion can exist only at the interface since it is insoluble in both the aqueous and organic phases. See text for more details.

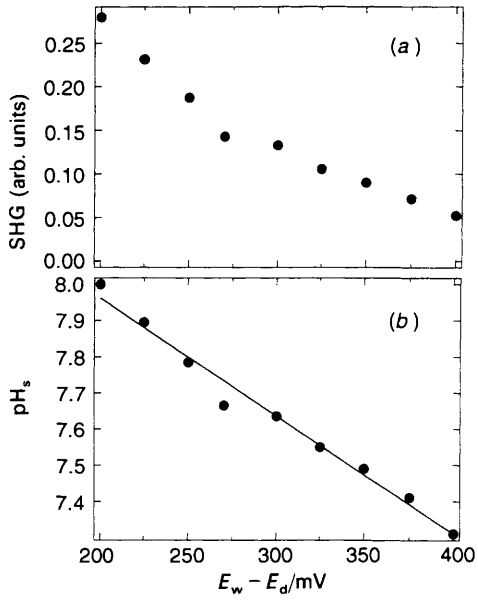


**Fig. 11** (*a*) Resonant molecular SHG signal from a monolayer of DBA at the water/DCE ITIES as a function of potential. The aqueous and DCE phases are the same solutions as those described in Fig. 8, with $pH_w = 8.0$. Surface tension measurements indicate that the pzc is at 220 mV for this interface; the decrease in SHG intensity at potentials positive of the pzc is in sharp contrast to the behaviour of the ONS anion shown in Fig. 7. From the SHG intensity, a relative surface coverage $\theta_{A_s^-}$ can be calculated. (*b*) Effective interfacial $pH_s$ corresponding to $\theta_{A_s^-}$ [as determined from eqn. (15)] as a function of potential. From the slope of this plot, a value of 0.19 for the ratio $\Delta\phi_{ws}/\Delta\phi_{wd}$ is obtained (see text for details).

this route in the bulk organic phase should be negligible. Furthermore, in the absence of current, no significant desorption of $A^-$ from the interface into the DCE can occur by ion transfer. All of the SHG measurements were performed in the window of no current for this interface.

Using a Langmuir isotherm relationship for $K_{ads}$ and $[DBA]_d$ in conjunction with the standard acid–base equilibrium for $K_a$ at the surface, results in the following equation for the relative surface, coverage of the DBA anion, $\theta_{A_s^-}$, at the water/DCE interface:

$$\theta_{A_s^-} = \left(1 + \frac{[H^+]_s}{K_{ads}K_a[DBA]_d}\right)^{-1} \quad (14)$$

In eqn. (14), $[H^+]_s$ is the hydrogen ion activity at the interface (or more precisely, at the position of the surfactant in the interface). If we assume that at open circuit $pH_s \approx pH_w$ (surface tension measurements suggest that this is true to within 0.05 pH units), then the data in Fig. 8 and 9 can be fitted to eqn. (14). The solid lines in the figures represent the best fit to the data with a $K_{ads}K_a$ product of $1.25 \times 10^{-3}$. The acid dissociation constant for a simple benzoic acid is $pK_a = 4.2$. If this same value is used for the azobenzene benzoic acid, a $K_{ads}$ of 20 $dm^3\ mol^{-1}$ is obtained (a very small adsorption constant). This low value is also supported by the fact that no neutral adsorption of DBA to the liquid/liquid interface at low $pH_w$ values was observed in this concentration range.

In a third set of resonant molecular SHG measurements, the resonant SHG from the monolayer of adsorbed DBA anions is obtained as a function of applied potential ($E_w - E_d$) at a $pH_w = 8.0$ and is plotted in Fig. 11(*a*). Recall that the relative surface coverage $\theta$ can be obtained from the square root of the SHG signal. No change in the polarization dependence of the SHG, and therefore the molecular orientation, was observed as a function of potential. A decrease in SHG is observed for potentials positive of the pzc (which is determined to be *ca.* 220 mV from surface tension measurements). This is in contrast to the adsorption behaviour of the anionic surfactant ONS (see Fig.7); the difference between these two adsorbate systems is confirmed by differences in the potential dependence of the interfacial surface tension for DBA and ONS.[53] Since DBA is adsorbed to the interface as a neutral species, the adsorption process involves no charge transport. Thus, the potential dependence of DBA adsorption is not as strongly affected by the double layer at the interface as in the case of ONS.

However, the applied potential does affect the interfacial $pH_s$. This interfacial $pH_s$ differs from the bulk aqueous $pH_w$ as a function of potential according to eqn. (15):[54,5]

$$pH_s = pH_w - \frac{F\Delta\phi_{ws}}{2.3RT} \quad (15)$$

where $\Delta\phi_{ws}$ is defined in Fig. 10 as the portion of the total potential drop ($\Delta\phi_{wd} \approx E_w - E_d$) that occurs from the aqueous phase to the position of the DBA anion within the interface. Through eqn. (14), the optically determined DBA relative surface coverage $\theta$ can be used to determine $pH_s$ as a function of applied potential. The results of this calculation are shown in Fig. 11(*b*), and demonstrate that $pH_s$ varies linearly with $\Delta\phi_{wd}$. However, the slope of this curve is not equal to $F/2.3RT$ (59 $mV^{-1}$) implying that $\Delta\phi_{ws} \neq \Delta\phi_{wd}$. Instead, the observed slope of 310 $mV^{-1}$ indicates that $\Delta\phi_{ws} \approx 0.19\Delta\phi_{wd}$, *ca.* 20% of the total interfacial potential difference, at an aqueous $pH_w = 8.0$. This result suggests that the DBA anion resides at the interface with a significant portion of the molecule in the aqueous region.

The ratio $\Delta\phi_{ws}/\Delta\phi_{wd}$ was found to vary as a function of aqueous $pH_w$; this variation is plotted for values of $pH_w$ between 7.5 and 8.3 in Fig. 12. A linear increase of $\Delta\phi_{ws}/\Delta\phi_{wd}$ with $pH_w$ is observed which can be explained in terms of a Helmholtz capacitor model of the interface. At potentials positive of the pzc, the aqueous side of the interface contains a 'plate' of positive charge composed primarily of $Na^+$ ions. On the DCE side of the interface resides a plate of negative charge composed mainly of tetraphenylborate ions. The DBA surfactant anions are a minor part of the negative charge on the interface at lower surface coverages. Their position in the interface is defined by the affinity of the parts of the molecule

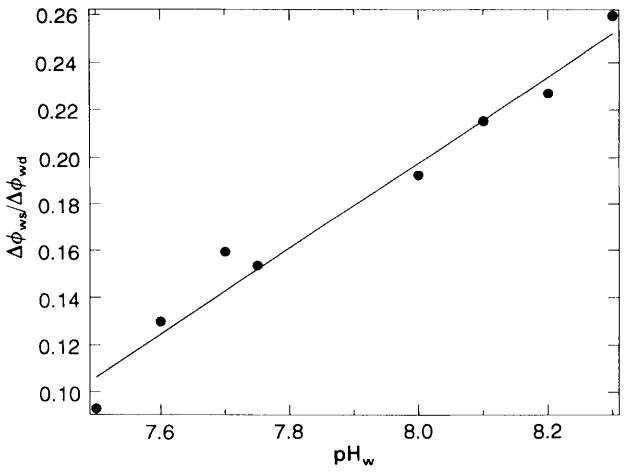


**Fig. 12** Plot of the ratio $\Delta\phi_{ws}/\Delta\phi_{wd}$ as a function of aqueous $pH_w$. This ratio increases as the $pH_w$ is raised since the DBA anion becomes a larger percentage of the charged double layer at the interface at higher $pH_w$ (see Fig. 8).

for the two different solvents, and this position in the interfacial capacitor determines the portion of the potential drop felt by the surfactant, and thus the interfacial $pH_s$ at the surfactant position. The value of 0.09 determined for the ratio $\Delta\phi_{ws}/\Delta\phi_{wd}$ at a $pH_w$ of 7.5 from the SHG measurements implies that the DBA anions are closer to the $Na^+$ ions and therefore further into the aqueous phase than the tetraphenylborate anions at the interface. As $pH_w$ is increased, the adsorbed DBA anions become a larger percentage of the negative plate of the capacitor. This implies that the effective position of the negative capacitor plate has moved closer to the DBA anions. The distance from the DBA anions to the positive plate is fixed by chemical sources, so that the $\Delta\phi_{ws}/\Delta\phi_{wd}$ ratio increases as the DBA surface coverage increases. Since the DBA surface coverage $\theta$ varies in an almost linear fashion in this $pH_w$ range (see Fig. 8), a linear increase in the ratio $\Delta\phi_{ws}/\Delta\phi_{wd}$ as a function of $pH_w$ is observed.

## 7. Summary and Conclusions

In this article we have demonstrated how molecular orientation and adsorption can be monitored at the ITIES with the non-linear spectroscopic technique of SHG. When the SHG from a liquid/liquid electrochemical interface is dominated by the resonant molecular contributions of an adsorbed SHG-active monolayer, the surface SHG signal can serve as an *in situ* measure of surfactant surface coverage as a function of solution concentration, aqueous pH and applied potential. Orientation information can be obtained by analysing the polarization dependence of the surface SHG, provided that the primary elements of the molecular non-linear polarizability tensor have been identified.

In the case of the weak acid surfactant DBA, SHG measurements demonstrate that adsorption to the water/DCE ITIES can be described by a combination of Langmuir adsorption and acid dissociation equilibria. At low surfactant concentrations in the DCE, the DBA resides at the interface in its anionic form at aqueous $pH_w$ values above 7.0. The surface coverage of the DBA anion as a function of applied potential can also be monitored with the surface SHG measurements, and is related to the interfacial $pH_s$ and the potential drop from the aqueous phase to the surfactant position within the ITIES. In future work, we will utilize the photochemical activity of DBA surfactant to study reactivity at the water/DCE ITIES.

The authors wish to thank the National Science Foundation for support of this work, and the Department of Defense for support through a National Defense Science and Engineering Graduate Fellowship (RRN).

## References

1 W. Nernst and E. H. Riesenfeld, *Ann. Phys.*, 1902, **8**, 600.
2 H. H. Girault and D. J. Schiffrin, *Electroanal. Chem.*, 1989, **15**, 1.
3 M. Senda, T. Kakiuchi and T. Osakai, *Electrochim. Acta*, 1991, **36**, 253.
4 Z. Samec, *Chem. Rev.*, 1988, **88**, 617.
5 V. Marecek, J. Koryta and Z. Samec, *Science*, 1988, **29**, 1.
6 P. Vanysek, *Electrochemistry on Liquid/Liquid Interfaces*, Springer-Verlag, Berlin, 1985.
7 H. H. Girault, *Electrochim. Acta*, 1987, **32**, 383.
8 J. Koryta, *Electrochim. Acta*, 1988, **33**, 189.
9 D. A. Higgins and R. M. Corn, *J. Phys. Chem.*, 1993, **97**, 489.
10 D. A. Higgins, R. R. Naujok and R. M. Corn, *Chem. Phys. Lett.*, 1993, **213**, 485.
11 K. L. Kott, D. A. Higgins, R. J. McMahon and R. M. Corn, *J. Am. Chem. Soc.*, 1993, **115**, 5342.
12 Y. R. Shen, *The Principles of Nonlinear Optics*, Wiley, New York, 1984.
13 R. M. Corn and D. A. Higgins, *Chem. Rev.*, 1994, **94**, 107.
14 K. B. Eisenthal, *Annu. Rev. Phys. Chem.*, 1992, **43**, 627.
15 T. F. Heinz, in *Nonlinear Surface Electromagnetic Phenomena*, ed. H. E. Ponath and G. I. Stegeman, North-Holland, Amsterdam, 1991, p. 353.
16 Y. R. Shen, *Annu. Rev. Phys. Chem.*, 1989, **40**, 327.
17 G. L. Richmond, in *Electroanalytical Chemistry*, ed. A. J. Bard, Marcel Dekker, New York, 1991, p. 87.
18 P. Guyot-Sionnest, W. Chen and Y. R. Shen, *Phys. Rev. B*, 1986, **33**, 8254.
19 M. C. Goh, J. M. Hicks, K. Kemnitz, G. R. Pinto, K. Bhattacharyya, K. B. Eisenthal and T. F. Heinz, *J. Phys. Chem.*, 1988, **92**, 5074.
20 J. M. Lantz and R. M. Corn, *J. Phys. Chem.*, 1994, **98**, 4899.
21 J. M. Lantz and R. M. Corn, *J. Phys. Chem.*, 1994, **98**, 9387.
22 D. A. Higgins, PhD Thesis, University of Wisconsin, 1993.
23 T. F. Heinz, C. K. Chen, D. Ricard and Y. R. Shen, *Phys. Rev. Lett.*, 1982, **48**, 478.
24 J. F. Ward, *Rev. Mod. Phys.*, 1965, **37**, 1.
25 D. Li, T. J. Marks and M. A. Ratner, *Chem. Phys. Lett.*, 1986, **131**, 370.
26 D. A. Higgins, M. B. Abrams, S. B. Byerly and R. M. Corn, *Langmuir*, 1992, **8**, 1994.
27 D. J. Campbell, D. A. Higgins and R. M. Corn, *J. Phys. Chem.*, 1990, **94**, 3681.
28 Z. Samec, V. Marecek and J. Weber, *J. Electroanal. Chem.*, 1979, **100**, 841.
29 J. D. Reid, O. R. Melroy and R. P. Buck, *J. Electroanal Chem.*, 1983, **147**, 71.
30 T. Nakanaga and T. Takenaka, *J. Phys. Chem.*, 1977, **81**, 645.
31 J. A. Oudar and J. Zyss, *Phys. Rev. A*, 1982, **26**, 2016.
32 J. Zyss and D. S. Chemla, in *Nonlinear Optical Properties of Organic Molecules and Crystals*, ed. D. S. Chemla and J. Zyss, 1987, p. 23.
33 B. F. Levine, *Chem. Phys. Lett.*, 1976, **37**, 516.
34 A. Ulman, *J. Phys. Chem.*, 1988, **92**, 2385.
35 T. F. Heinz, H. W. K. Tom and Y. R. Shen, *Phys. Rev. A*, 1983, **28**, 1883.
36 D. A. Higgins, S. K. Byerly, M. B. Abrams and R. M. Corn, *J. Phys. Chem.*, 1991, **95**, 6984.
37 R. M. Corn and D. A. Higgins, in *Characterization of Organic Thin Films*, ed. A. Ulman, Butterworth-Heineman, 1995, p. 227.
38 A. J. Bell, J. G. Frey and T. J. VanderNoot, *J. Chem. Soc., Faraday Trans.*, 1992, **88**, 2027.
39 R. Pariser and R. G. Parr, *J. Chem. Phys.*, 1953, **21**, 466.
40 J. A. Pople, *Trans. Faraday Soc.*, 1953, **49**, 1375.
41 D. Li, M. A. Ratner and T. J. Marks, *J. Am. Chem. Soc.*, 1988, **110**, 1707.
42 I. D. L. Albert, P. K. Das and S. Ramasesha, *Chem. Phys. Lett.*, 1986, **168**, 454.
43 S. Ramasesha and P. K. Das, *Chem. Phys.*, 1990, **145**, 343.
44 T. G. Zhang, C. H. Zhang and G. K. Wong, *J. Opt. Soc. Am., B*, 1990, **7**, 902.
45 S. G. Grubb, M. W. Kim, T. Rasing and Y. R. Shen, *Langmuir*, 1988, **4**, 452.

46 V. Mizrahi and J. E. Sipe, *J. Opt. Soc. Am., B*, 1988, **5**, 660.
47 *Handbook of Chemistry and Physics*, ed. D. R. Lide, CRC Press, Ann Arbor, 1991.
48 P. Guyot-Sionnest, Y. R. Shen and T. F. Heinz, *Appl. Phys. B*, 1987, **42**, 237.
49 T. L. Mazely and W. M. I. Hetherington, *J. Chem. Phys.*, 1987, **86**, 3640.
50 A. J. Bard and L. R. Faulkner, *Electrochemical Methods: Fundamentals and Applications*, Wiley, Toronto, 1980.
51 T. Kakiuchi and M. Senda, *Bull. Chem. Soc. Jpn.*, 1983, **56**, 1322.
52 V. S. Bagotzky, *Fundamentals of Electrochemistry*, Plenum Press, New York, 1993.
53 R. R. Naujok and R M. Corn, unpublished results.
54 X. Zhao, S. Subrahmanyan and K. B. Eisenthal, *Chem. Phys. Lett.*, 1990, **171**, 558.
55 X. Zhao, S. Ong, H. Wang and K. B. Eisenthal, *Chem. Phys. Lett.*, 1993, **214**, 203.

*Paper* 4/07689C; *Received* 16*th December*, 1994